A theoretical study on thermoelectric properties of graphene nanoribbons

Yijian Ouyang and Jing Guo[a)]
Department of Electrical and Computer Engineering, University of Florida, Gainesville, Florida 32611, USA

(Received 23 April 2009; accepted 4 June 2009; published online 30 June 2009)

We investigate the thermoelectric properties of graphene nanoribbons (GNRs) by solving atomistic electron and phonon transport equations in the nonequilibrium Green's function formalism. The dependence of thermopower on temperature and chemical potential is compared to that of graphene, which shows the important role of quasi-one-dimensional geometry in determining the thermoelectric properties of a GNR. The edge roughness and lattice vacancy are found to increase the thermopower but decrease the thermoelectric *ZT* factor because the decrease in the electronic conductance outweighs the decrease in the thermal conductance and the increase in the thermopower. © *2009 American Institute of Physics*. [DOI: 10.1063/1.3171933]

The discovery of the two-dimensional (2D) graphene and quasi-one-dimensional (1D) graphene nanoribbon (GNR) has attracted strong interest in their fundamental physical properties and potential device applications.[1–3] The thermoelectric transport properties, which reveal electron and phonon transport properties, have been examined by studying the electronic and thermal transport characteristics of the 2D graphene experimentally and theoretically.[4–6] But the thermoelectric transport properties of GNRs remain unclear. In silicon thermoelectricity, the thermoelectric *ZT* factor increases by orders of magnitude compared to bulk silicon for a silicon nanowire with rough surface.[7–9] By comparing to 2D graphene, it is interesting to understand how quasi-1D structure and edge roughness of a GNR affect its thermoelectric properties.

In this letter, we investigate the thermoelectric properties of GNRs by solving the electronic transport and thermal transport equations in the nonequilibrium Green's function (NEGF) formalism. By computing the electronic conductance G_e, thermal conductance κ, and thermopower S, we obtain the figure of merit ZT defined by $ZT \equiv TG_eS^2/\kappa$, where T is temperature. We found that for semiconducting GNRs, the ZT factor is maximized when the chemical potential is near the first subband edge. The maximum magnitude of thermopower, which is reached with the chemical potential near the middle of the band gap, is inversely proportional to temperature and is much larger than that of the 2D graphene due to the presence of the band gap. When the chemical potential moves above the band edge, the thermopower decreases to zero because of the stepwise 1D transmission spectrum. The edge roughness and lattice vacancy defects increase the thermopower but decrease the ZT factor.

For electronic transport, the Hamiltonian is described by an atomistic p_Z orbital tight binding basis with nearest coupling. The semi-infinite GNR source and drain leads are defect-free. The retarded Green's function of the channel is calculated as[10]

$$G(E) = [(E + i0^+)I - H - \Sigma_1 - \Sigma_2]^{-1}, \tag{1}$$

where H is the unperturbed channel Hamiltonian matrix and Σ_1 (Σ_2) is the self-energy due to the semi-infinite source (drain) lead. The electronic transmission per spin through channel region is calculated as

$$T_e(E) = \mathrm{Tr}[\Gamma_1(E)G(E)\Gamma_2(E)G^+(E)], \tag{2}$$

where $\Gamma_{1,2} = -2\ \mathrm{Im}(\Sigma_{1,2})$ is the broadening function of source (drain) lead and G^+ is the advanced Green's function. NEGF formalism can rigorously treat the transport through the channel with translational symmetry breaking (e.g., by defects). Due to the weak electron-phonon coupling in GNRs, phonon scattering of electrons is neglected.[11] The electronic conductance, thermopower, and the electronic contribution to the thermal conductance κ_e can be conveniently derived from the electronic transmission by defining an intermediate function $L_n(\mu)$ as

$$L_n(\mu,T) = \frac{2}{h}\int dE T_e(E)(E-\mu)^n\left[-\frac{\partial f(E,\mu,T)}{\partial E}\right], \tag{3}$$

where h is the Plank constant, the factor 2 counts the spin degeneracy, and f is the Fermi distribution function. G_e, S, and κ_e are computed as[12]

$$G_e(\mu) = e^2 L_0(\mu,T), \tag{4}$$

$$S(\mu) = \frac{1}{qT}\frac{L_1(\mu,T)}{L_0(\mu,T)}, \tag{5}$$

$$\kappa_e(\mu) = \frac{1}{T}\left[L_2(\mu,T) - \frac{L_1(\mu,T)^2}{L_0(\mu,T)}\right], \tag{6}$$

where q is the electric charge of carriers, which is positive for holes and negative for electrons.

The Green's function and transmission can be calculated similarly for phonon transport.[13] In Eq. (1) one only needs to change E to $\omega^2 M$, H to D, and compute the self-energies accordingly, where ω is the phonon frequency, M is the atomic mass of carbon, and D is the dynamic matrix. The dynamic matrix only includes carbon atoms as the hydrogen atoms at the edges are not important in forming vibration modes.[14] The dynamic matrix is constructed by using a spring mass model.[15] The lattice contribution to the thermal conductance is given by

a)Electronic mail: guoj@ufl.edu.

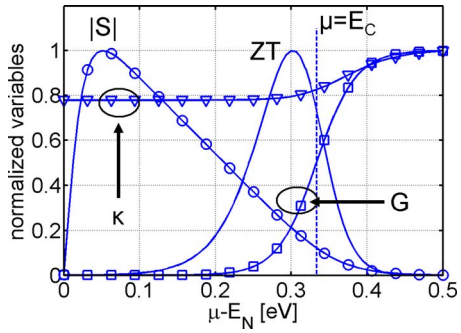

FIG. 1. (Color online) Normalized ZT, $|S|$, κ, and G of a perfect $n=15$ AGNR as functions of the chemical potential μ. The energy reference point ($E=0$) is defined as the middle of the band gap. $S<0$ for $\mu>0$ (i.e., electron conduction). The values are normalized by $ZT_0=0.109$, $G_0=77.1$ μS, $\kappa_0=2.52\times10^{-9}$ W/K, and $S_0=981$ μV/K, respectively.

$$\kappa_{\mathrm{ph}}=\frac{1}{h}\int d\hbar\omega T_{\mathrm{ph}}(\omega)\hbar\omega\left[\frac{\partial n(\omega)}{\partial T}\right], \tag{7}$$

where T_{ph} is the phonon transmission and $n(\omega)$ is the Bose–Einstein distribution function. Phonon-phonon scattering and a harmonic lattice vibration are ignored.

We first investigate the thermoelectric properties of a structurally perfect armchair edge GNR (AGNR). The modeled AGNR has an index of $n=15$, which results in a width of 1.8 nm and a band gap of $E_g=667$ meV. The chemical potential of the GNR can be tuned with gating or doping. Therefore we investigate the dependence of the electronic conductance, thermal conductance, thermopower, and the ZT factor as functions of the chemical potential. As shown in Fig. 1, as the chemical potential moves into conduction subbands, the electronic conductance increases because more subbands are available for conduction. An increase in the electronic conductance also increases the electronic contribution to the thermal conductance. In contrast, the thermal conductance does not change much by varying the position of the chemical potential because the constant lattice contribution dominates the thermal conductance. Both the thermopower and the ZT factor show a distinctive peak. To understand the peak on the thermopower curve, one can inspect Eq. (5) which indicates that S is determined by the electron-transmission-weighted average value of the heat energy E-μ. The thermopower S is zero when the chemical potential is at the middle of the band gap $\mu=0$ due to the symmetric conduction and valence subbands. For electron conduction ($S<0$), the maximum $|S|$ occurs when the chemical potential is several k_BT above the middle of the band gap. This is the position where the electron-transmission-weighted average value of (E-μ) is maximized. Compared to the $|S|$ peak, the ZT peak is reached at a totally different chemical potential, which is close to the subband edge. This is because the electronic conductance decreases exponentially as the chemical potential moves several k_BT below the conduction band edge. The thermopower decreases as the chemical potential moves above the band edge where electronic transmission becomes energy independent. So the maximum value of $ZT=TG_eS^2/\kappa$ is reached with the chemical potential near the subband edge.

Next, we compare the thermoelectric properties of the GNR to 2D ballistic graphene. We plot the thermopower of the GNR and 2D graphene as a function of the chemical potential at different temperatures in Figs. 2(a) and 2(b), respectively. The thermopower of graphene is calculated without scattering, which represents the ballistic transport limit and warrants a fair comparison to the modeled GNR characteristics. For 2D graphene, as shown in Fig. 2, the simulated S versus μ curve is qualitatively similar to the experiment in terms of its antisymmetric shape to the Dirac point.[4] The peak value of S simulated at the ballistic limit is also close to the experimental value,[4] although scattering can be responsible for a different dependence of the peak values on temperature in the experiment. By comparing the thermopower curves of the GNR to those of the graphene, some important similarities and differences can be identified. For both the graphene and GNR, the curves are similar in terms of being antisymmetric about the Dirac point (or the middle of the band gap E_m) due to the symmetrical band structures, and both curves have the maximum thermopower when the chemical potential is several k_BT away from E_m. One major difference is that the maximum magnitude of the thermopower of the GNR, which is in the order of mV/K, is much larger than that of graphene, which is less than 100 μV/K. This is mainly due to the existence of the band gap in semiconducting GNR, so that the electrons at the conduction subband edge, which are responsible for electron conduction at the maximum thermopower, have a much larger (E-μ) compared to the gapless 2D graphene.

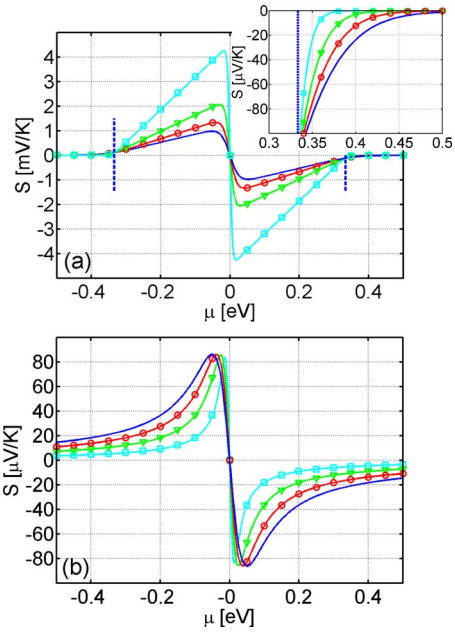

FIG. 2. (Color online) Compare 1D GNR to 2D graphene: the thermopower of (a) a perfect $n=15$ AGNR and (b) a 2D graphene as a function of μ at different temperatures: $T=75$ K (squares), 150 K (triangles), 225 K (circles), and 300 K (unmarked). In (a) the dashed line indicates the first conduction subband edge E_C. The inset shows the enlarged parts for $\mu>E_C$.

For electron conduction, when the chemical potential is between the middle of the band gap and the conduction band edge ($0<\mu<E_C-3k_BT$), it can be shown that the average heat energy $L_1(\mu)/L_0(\mu)\approx E_C$-$\mu$ by using nondegenerate Maxwell–Boltzmann carrier distribution, and the magnitude of the thermopower is $|S|\approx(E_C$-$\mu)/Te$. As a result, the average heat energy can be up to one half of the band gap. For $n=15$ AGNR, $E_g/2=334$ meV, and thus the thermopower can be in the order of mV/K. As shown in Fig. 2(a), the thermopower is approximately inversely proportional to the

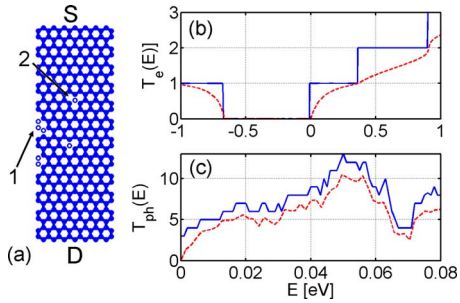

FIG. 3. (Color online) (a) The atomistic structure of an $n=15$ AGNR. Two types of defects are simulated: edge roughness as shown by arrow 1 and lattice vacancy as shown by arrow 2. The source (S) and drain (D) leads are perfect semi-infinite GNRs. (b) The electronic transmissions of the perfect AGNR (solid line) and the AGNR with one edge roughness defect (dashed line) as shown in arrow 1 of (a). (c) The phonon transmissions of a perfect GNR (solid line) and the same defective structure as in (b) (dashed line).

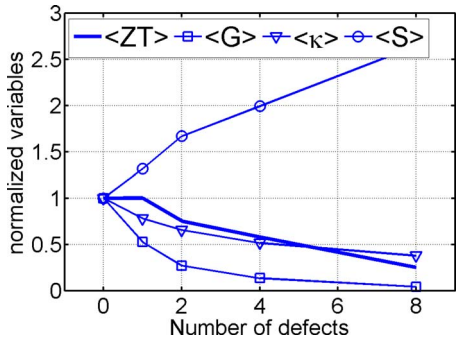

FIG. 4. (Color online) Effect of edge and lattice vacancy defects: the normalized sample-averaged $\langle ZT\rangle$, thermopower $\langle S\rangle$, thermal conductance $\langle\kappa\rangle$, and electronic conductance $\langle G_e\rangle$ as functions of the number of defects in the $n=15$ AGNR. The values are normalized by $ZT_0=0.10$, $G_0=38.6$ μS, $\kappa_0=1.66\times10^{-9}$ W/K, and $S_0=120$ μV/K, respectively. The chemical potential is fixed at the first conduction subband edge.

temperature when nondegenerate carrier statistics applies. For graphene, since the band gap is zero, only the carriers within several k_BT about the chemical potential are important for transport. Thus the average heat energy is in the order of k_BT, which results in a much smaller thermopower. It can be shown that when the chemical potential is several k_BT above the Dirac point, the thermopower approximately scales as $T/(\mu\text{-}E_m)$, which is proportional to the temperature. This difference in temperature dependence between the graphene and GNR is purely due to the existence of the band gap in the GNR.

When the chemical potential in the GNR moves into conduction bands, $|S|$ of the GNR decreases to zero, which is distinctively different from that of the graphene. This is because the quasi-1D GNR has a stepwise transmission spectrum. When the chemical potential moves into the conduction (valence) bands, the transmission is energy independent before the chemical potential reaching the next subband, which results in a zero thermopower. In contrast, the 2D graphene has a transmission linearly dependent on the energy. The energy-dependent transmission leads to a nonzero S. The very different dependence of the thermopower on the chemical potential is caused by the difference between transmission spectra of the quasi-1D GNR and 2D graphene.

Finally, we examine the effect of edge roughness and lattice vacancy. The defects are treated by removing the carbon atoms out of the channel, which results in vacancy in bulk region and roughness at edges, as shown in Fig. 3(a). Any dangling bonds arising from missing carbon atoms are assumed to be passivated by a hydrogen atom to keep the tight-binding prescription valid. The sample-averaged value is obtained by averaging a physical quantity over 100 GNRs with randomly generated defects.

To lustrate the effect of the lattice defects, one edge roughness defect is introduced to the channel. The stepwise transmission of the perfect structure is degraded and smoothed for both electron transport [Fig. 3(b)] and phonon transport [Fig. 3(c)] due to the translational symmetry breaking. As the number of defects increases, the transmissions decrease which lead the electronic conductance and thermal conductance to decrease, as shown in Fig. 4. However the magnitude of the thermopower increases as the number of defects increases. This can be explained by analyzing Eq. (5) together with Eq. (3). At a given temperature, the thermopower, Eq. (5), is proportional to the transmission-weighted average heat energy $(E\text{-}\mu)$. Carriers of a higher energy E carry a larger magnitude of heat energy. To increase the thermopower, the low energy carrier transport should be suppressed. By smoothing the sharp corner at conduction band edge in the perfect transmission spectrum, the electronic transport near the band edge, where carrier energy is low, is effectively reduced and the weight of high energy carriers in total carriers is increased. Therefore the magnitude of the thermopower increases as the GNR becomes more defective. Although both the increase in the thermopower and the decrease in the thermal conductance can increase the ZT factor, the degradation of the electronic conductance outweighs them and the ZT factor decreases as the number of defects increases.

In summary we have presented an atomistic simulation for the electronic and thermal transport of the GNR in NEGF formalism. The dependence of the thermoelectric properties on temperature, chemical potential, and defects is investigated. The thermopower characteristics are compared to that of the 2D graphene which reveals the important role of the quasi-1D geometry in determining the thermoelectric properties of the GNR.

This work was supported by NSF and ONR. The computational resources were supported in part by the University of Florida High Performance Computing Center.

[1] K. S. Novoselov, A. K. Geim, S. V. Morozov, D. Jiang, Y. Zhang, S. V. Dubonos, I. V. Grigorieva, and A. A. Firsov, Science **306**, 666 (2004).
[2] Y. B. Zhang, Y. W. Tan, H. L. Stormer, and P. Kim, Nature (London) **438**, 201 (2005).
[3] X. Li, X. Wang, L. Zhang, S. Lee, and H. Dai, Science **319**, 1229 (2008).
[4] Y. M. Zuev, W. Chang, and P. Kim, Phys. Rev. Lett. **102**, 096807 (2009).
[5] T. Lofwander and M. Fogelstrom, Phys. Rev. B **76**, 193401 (2007).
[6] E. H. Hwang, E. Rossi, and S. Das Sarma, arXiv:0902.1749v1.
[7] A. I. Hochbaum, R. Chen, R. D. Delgado, W. Liang, E. C. Garnett, M. Najarian, A. Majumdar, and P. Yang, Nature (London) **451**, 163 (2008).
[8] A. I. Boukai, Y. Bunimovich, J. Tahir-Kheli, J.-K. Yu, W. A. Goddard III, and J. R. Heath, Nature (London) **451**, 168 (2008).
[9] T. Markussen, A. P. Jauho, and M. Brandbyge, Phys. Rev. B **79**, 035415 (2009).
[10] S. Datta, *Quantum Transport: Atom to Transistor* (Cambridge University Press, Cambridge, England, 2005).
[11] D. Gunlycke, H. M. Lawler, and C. T. White, Phys. Rev. B **75**, 085418 (2007).
[12] U. Sivan and Y. Imry, Phys. Rev. B **33**, 551 (1986).
[13] T. Yamamoto and K. Watanabe, Phys. Rev. Lett. **96**, 255503 (2006).
[14] T. Markussen, A. P. Jauho, and M. Brandbyge, Nano Lett. **8**, 3771 (2008).
[15] R. Saito, G. Dresselhaus, and M. S. Dresselhaus, *Physical Properties of Carbon Nanotubes* (Imperial College Press, UK, 2004).